Ecological Engineering 105 (2017) 231–239

Contents lists available at ScienceDirect

Ecological Engineering

journal homepage: www.elsevier.com/locate/ecoleng

Soil CO_2 emissions from different slope gradients and positions in the semiarid Loess Plateau of China

Zhiqi Wang[a,c], Rui Wang[b], Qiqi Sun[a], Lanlan Du[a], Man Zhao[b], Yaxian Hu[a], Shengli Guo[a,b,*]

[a] State Key Laboratory of Soil Erosion and Dryland Farming on the Loess Plateau, Institute of Soil and Water Conservation, Northwest A&F University, Yangling, Shaanxi 712100, China
[b] College of Resources and Environment, Northwest A&F University, Yangling 712100, China
[c] School of Resources and Environment, North China University of Water Resources and Electric Power, Zhengzhou 450045, China

ARTICLE INFO

Article history:
Received 8 August 2016
Received in revised form 30 March 2017
Accepted 27 April 2017
Available online 11 May 2017

Keywords:
CO_2 emissions
Runoff
Sediment
Slope position
Slope gradient

ABSTRACT

Knowledge of CO_2 emissions under different slope gradients and positions and its controlling factors is critical in accurately estimating CO_2 emissions and carbon cycling on the slopes of eroded regions. In this study, three east-facing plots of 100 m^2 (20 m × 5 m) with a slope gradient of 0.5° ($S_{0.5}$), 1° (S_1), and 3° (S_3) were established in an eroded gully of the semi-arid Loess Plateau, China. The CO_2 emission, temperature, moisture, runoff, sediment, fine root biomass and grain yield of these three plots were measured from October 2013 to September 2015 to investigate the relationship between slope gradients and soil CO_2 emissions. The results showed that the mean annual cumulative CO_2 emissions at S_1 and S_3 (731.0 ± 65.1 and 628.3 ± 74.8 g C m^{-2} $year^{-1}$) were about 13.4% and 25.5% lower than that at $S_{0.5}$ (843.7 ± 84.9 g C m^{-2} $year^{-1}$). The CO_2 emissions were higher at bottom slope than at upper slope, with an increase of 26.2% at S_3, 22.9% at S_1 and 14.5% at $S_{0.5}$, respectively. The mean soil moisture ranged from 40.8% to 44.8% water-filled pore space (WFPS) among the slope gradients, and from 35.8% to 45.6% WFPS among the slope positions. There was a significant difference in mean fine root biomass among different slope gradients ($S_{0.5} > S_1 > S_3$, $P < 0.05$), but no significant difference among different slope positions. The mean soil organic carbon (SOC) ranged from 8.8 g kg^{-1} at S_3 to 9.9 g kg^{-1} at $S_{0.5}$, and that at the bottom and middle slope were higher than that at the upper slope at S_1 and S_3. Slope differentiated soil moisture content and redistribution, and the thus derived spatial differences in fine root biomass and crop yields, was the major factor influencing the soil CO_2 emissions among slope gradients and positions. Slope gradients and positions should be considered when estimating soil CO_2 emissions and carbon cycling in the complex and fragmented topography regions.

Highlights
•The soil CO2 emissions significantly decreased with the increase of slope gradient.
•The soil CO2 emissions were greater at the upper slope than at the bottom slope.
•The erosion-induced spatial redistribution of soil moisture and SOC, and the thus derived differences in fine root biomass and crop yield, lead to the differences in soil CO2 emissions across different slope gradients and positions

1. Introduction

Soil CO_2 emission is an important component of global carbon cycle, and even a small variation in soil respiration can have a significant effect on the atmospheric CO_2 concentration and soil organic carbon (SOC) stock (Bond-Lamberty and Thomson, 2010; Hursh et al., 2017). However, the potential effect of slope gradients and positions on soil CO_2 emissions has not yet been fully elucidated (Chen et al., 2015; Van Hemelryck et al., 2011). In fact, more than 60% of global land areas are slopes of > 8° (Berhe and Kleber, 2013). Slope gradients can not only affect soil water and heat at the slopes, but also change soil properties and vegetation (Fehmi and Kong, 2012; Wei et al., 2014; Xiao et al., 2015). Therefore, knowledge of the effect of slope land on soil CO_2 emissions is essential for a better understanding of the global atmospheric CO_2 budget and climate change.

Soil CO_2 emissions in sloping land can be particularly affected by the spatial distribution of soil moisture (Liu et al., 2016; Singh et al., 2017), SOC (Fereidoonia et al., 2013; Hursh et al., 2017) and fine root biomass (Makita et al., 2016; Pandey et al., 2016) at different positions of the slope. To be specific, soil moisture in sloping land was reported to be significantly lower than that on plains, mostly because of the increased loss of runoff and, consequently, a reduction in infiltration (Zhang et al., 2015a; Zhao et al., 2015). Soil moisture varied spatially along the slope and it was

* Corresponding author at: Institute of Soil and Water Conservation, Xinong Road 26, Yangling, Shaanxi 712100, China.
E-mail address: slguo@ms.iswc.ac.cn (S. Guo).

http://dx.doi.org/10.1016/j.ecoleng.2017.04.050
0925-8574/

significantly higher at the toe of the slope than at the summit (Wei et al., 2014). In consequence, the spatial difference in soil moisture at different slope positions may have considerable impacts on CO_2 emissions. In addition, SOC, as the main substrate for microbial organisms, can also differ spatially along the slope due to the selective or non-selective erosion effects (Pei et al., 2012; Van et al., 2010). For instance, SOC at the upper slope where soil was severely eroded was 9.1% lower than that at the middle slope where soil was mildly eroded, and 13.8% lower than that at the bottom slope where soil was deposited in a severely eroded slope land (Li et al., 2015b). Fine root biomass can reflect the varying biotic conditions at different slope positions, and decreases in an order of upper < middle < bottom in a *Pinus tabuliformis* forest at the south slope of *Qinling* Mountains of China (Liu et al., 2004). However, there have been no systematic studies investigating the effects of soil moisture, temperature, root biomass, grain yield and SOC under different slope gradients and positions on soil CO_2 emissions.

The main purpose of this study was to investigate whether soil CO_2 emissions at different slope gradients and positions were related to erosion-induced variations of water, crop growth and SOC. To address this problem, we compared CO_2 emissions at different positions (bottom, middle and upper slope) on the slopes of different gradients, and evaluated the potential effects of slope differentiated water, crop growth and SOC on CO_2 emissions at an eroded slope.

2. Materials and methods

2.1. Study area

In the semi-arid Loess Plateau, China, the area of arable land is 14.5×10^4 km^2. Tableland, steep slope and gully are the major topographical features of the Loess Plateau, each accounting for about one third of the watershed area. The tableland with a gentle slope (<5°) has a high nutrient content and thus has been the primary site for residence and agricultural production (Zhang et al., 2015b). However, these slopes are subject to serious water and soil loss due to the poor resistance to water erosion and the intensive cultivation (Jiang et al., 2015), thus resulting in gradually steeper slopes cutting into the edges of the tableland and a significant reduction in the tableland area (Chen et al., 2009).

The study area is located in the State Key Agro-Ecological Experimental Station, Wangdonggou (35°13′ N–35°16′ N, 107°40′ E–107°42′ E), Changwu county, Shaanxi province, China, which is a typical eroded gully (altitude: 1220 m) of the south Loess Plateau (Fig. 1). This area has a continental monsoon climate with an annual mean precipitation of 560 mm for the period 1984–2014 (523 mm in 2013 and 597 mm in 2014 during the measurement period), 60% of which occurs between July and September (Zhang et al., 2015b). Over 70% of the crops (wheat and corn) are planted in rain-fed areas, which are highly susceptible to climate change impacts (Jiang et al., 2015). In general, the soil erosion is serious in the study area with a soil erosion modulus of 2860 t km^{-2} a^{-1}, which has a detrimental effect on the crop yield, surface water quality and regional hydrological regimes (Zhu et al., 2014). This makes it suitable to investigate the potential effect of soil erosion along different slope gradients on CO_2 emissions.

2.2. Experimental design

2.2.1. Arrangement of plots

Three east-facing rectangular plots, each with an area of 100 m^2 (20 m × 5 m), and three slope gradients of 0.5° ($S_{0.5}$), 1° (S_1) and 3° (S_3) were established in the study area in 1998. Since then, all the plots have been planted with winter wheat every year. In order to make the experimental conditions as identical as possible, the plots were prepared following the same procedure. To be specific, all plots were filled with surface soil (0–20 cm) collected from the

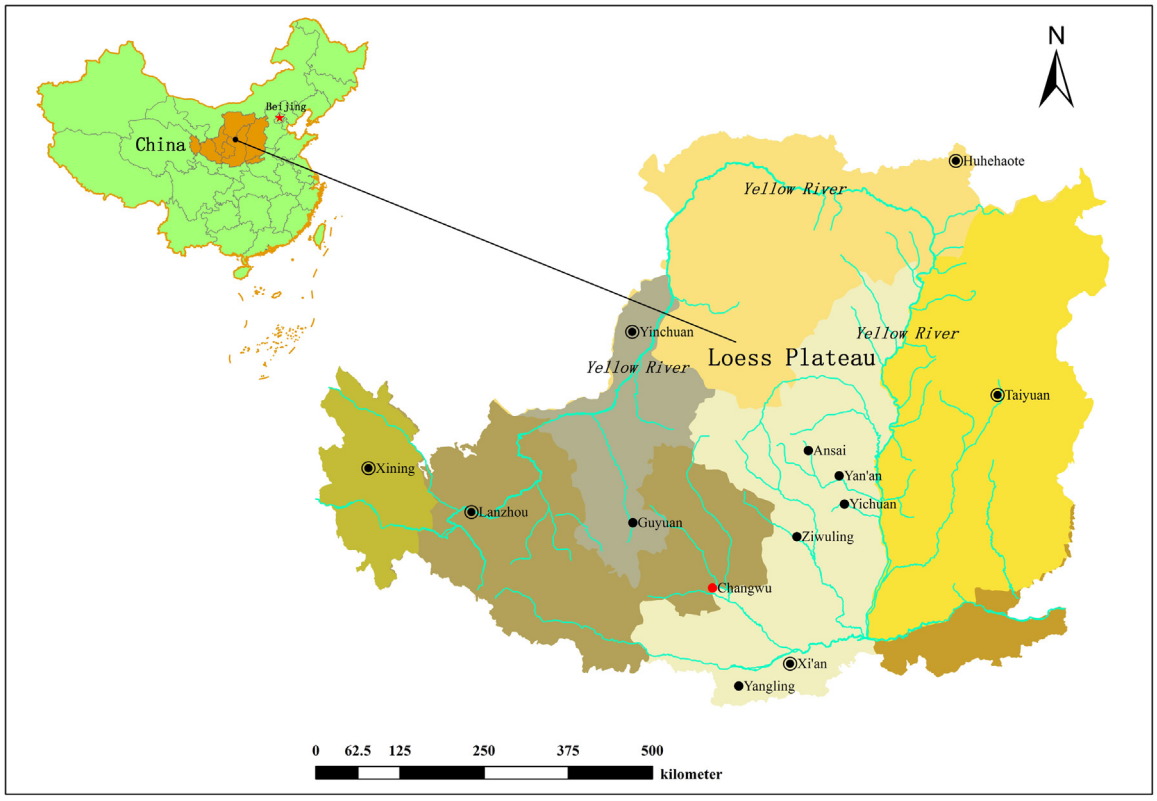

Fig. 1. A sketch map of the Loess Plateau.

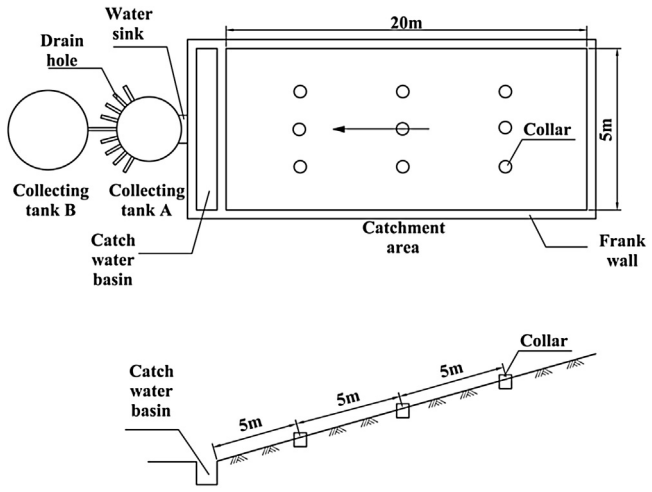

Fig. 2. The sketch map of the plots and location of PVC collars.

same local cropland in the tableland, and the soil bulk density was controlled at 1.30 g cm^{-3} and the soil moisture was controlled at 12–15%. The soil surface was carefully managed, without readily visible clods or depressions on each plot. At the beginning of this long-term experiment, the soil was the Loessi-Orthic Primosols (USDA Soil Taxonomy) and Cambisols (WRB) (Wang et al., 2015b), with a pH of 8.2, field capacity of 22.4%, permanent wilting point of 9.0%, SOC of 9.53 g kg^{-1}, total nitrogen (TN) of 0.99 g kg^{-1}, alkaline nitrogen of 37.0 mg kg^{-1}, available phosphorous of 3.0 mg kg^{-1}, available potassium of 129.3 mg kg^{-1}, clay content (<0.002 mm) of 24%, and $CaCO_3$ content of 12.6%.

Plots were spaced 0.5 m apart and separated by a brick wall of 15 cm in height, 40 cm in depth and 6 cm in thickness (Fig. 2) to prevent the inflow of runoff outside the plots and the outflow of runoff inside the plots. Each plot had a catchment water base, a water sink, and two water tanks (A and B) for the measurement of runoff and sediment. The water base was tilted inwardly towards the center to help water and sediment produced in the plot flow into the water sink. Two cylindrical steel buckets with an inner diameter of 80 and 90 cm and a height of 125 cm were used as the water tanks. Nine holes with the same diameter were arranged at a depth of 40 cm in water tank A. The middle hole was connected to water tank B, and the other eight holes were arranged symmetrically for the drainage of water.

Given that winter wheat is sown in October and harvested in June in the Loess Plateau, the year of 2014 refers to the period from October 1, 2013 to September 30, 2014 in this study; and similarly, the year of 2015 refers to the period from October 1, 2014 to September 30, 2015. During the summer fallow period, all plots were tilled by hand-hoeing to a depth of 20 cm and kept bare. Fertilizers were applied at a rate of 120 kg ha^{-1} N and 13 kg ha^{-1} P for each plot prior to planting, and broadcast and incorporated after 5–7 days at a depth of 20 cm prior to sowing. Weeds were removed manually, and field management was applied as required. All crops were harvested manually (the stubble height was about 5 cm), and all harvested biomass and leaf litter were removed from the plots at physiological maturity each year.

2.2.2. Measurement of soil CO_2 emissions, temperature and moisture

Soil CO_2 emissions were measured by three collars at each position of the slope (upper, middle and bottom) from 09:00 am to 11:00 am about every 10 days from October 1, 2013 to September 30, 2015 (Fig. 2). Soil CO_2 emission rate was measured twice for each plot with a 90 s enclosure period and a 30 s delay between the two measurements using an automated closed soil CO_2 emission system equipped with a portable chamber (20 cm in diameter; Li-8100, Lincoln, NE, USA). In order to avoid the potential bias of CO_2 emissions caused by the installation of collars, a polyvinyl chloride (PVC) collar (20 cm in diameter by 5 cm in height) was inserted 3 cm deep into each plot approximately one day in advance, to ensure a stabilized CO_2 emission rate on the measuring day. All visible living organisms were removed before the measurements. If necessary, one or more additional measurements were performed until the variation between two consecutive measurements was less than 15%. The final instantaneous soil CO_2 emissions for a given collar was the average of the two consecutive measurements.

Soil temperature (three measurements per collar) and moisture (four measurements per collar) at a depth of 5 cm and a distance of 10 cm from the collar were measured at the same time as the soil CO_2 emissions using Li-Cor thermocouple probe and Theta Probe ML2X with an HH2 moisture meter (Delta-T Devices, Cambridge, England), respectively. Soil water-filled pore space (WFPS) was calculated by the following equation:

$$WFPS(\%) = V/100 \times (2.65 - B)/2.65 \quad (1)$$

where WFPS (%) is the soil water-filled pore space, V is the volumetric water content (%), and B is the bulk density (g cm^{-3}).

2.2.3. Measurement of fine root biomass, grain yield and SOC

Three soil cores (9 cm in diameter and 20 cm in height) at 0–20 cm depths at each position were collected in permeable nylon bag at each harvest season, and then flushed with water to obtain fine root and oven-dried to a constant weight at 60 °C for 48 h. Fine root (<2 mm in diameter) biomass was collected and measured to determine the cumulative root biomass over the growing season. The grain yield was measured per unit area (m^2).

Soils in the 0–5 cm soil profiles were sampled for SOC measurement using a soil auger with a diameter of 3 cm (3 replicates per plot) in 2015. A total of nine samples were obtained at each gradient, with three samples at each position. The soil samples were mixed evenly, air dried, and then crushed to pass through a 0.15 mm sieve (Zhang et al., 2015b). SOC was determined using the K_2CrO_7-H_2SO_4 oxidation method (Sparks et al., 1996).

2.3. Data analysis

The effects of slope gradients and positions on soil CO_2 emissions, temperature, moisture, runoff, sediment, fine root biomass and yield were analyzed by the GLM procedure using the SAS software. A quadratic polynomial function was used to simulate the relationship between soil CO_2 emissions and soil moisture (Tang et al., 2005). The mean daily soil respiration for each plot was interpolated between measurement dates, and then the annual cumulative soil respiration was calculated.

3. Results

3.1. Runoff, sediment and SOC

In both 2014 and 2015, the runoff and sediment yield increased with increasing slope gradients ($P < 0.05$; Table 1). The maximum annual runoff was observed at S_3 (0.313 and 0.259 m^3 in 2014 and 2015, respectively), while the sediment yield no significant difference. The SOC concentration on the slopes followed the order of $S_{0.5} > S_1 > S_3$ in 2015 ($P < 0.05$; Table 2). In addition, the SOC concentration at S_3 and S_1 followed the order of bottom > middle > upper ($P < 0.05$); while there was no significant difference in the SOC concentration at $S_{0.5}$ ($P > 0.05$; Table 2).

Table 1
Rainfall, runoff and sediment amount at the three slope gradients over a 2-year period.

Slope gradient (°)	Runoff (m^3)	Sediment concentration ($kg\,m^{-3}$)	Amount of soil erosion ($Mg\,ha^{-1}$)	Rainfall (mm-date)
3	0.038	0.029	0.003	39.2
1	0.012	0.062	0.006	(2013–7-
0.5	0.004	0.001	0	11)
3	0.044	0.021	0.002	60.6
1	0.017	0.016	0.002	(2013–7-
0.5	0.008	0.008	0.001	20)
3	0.231	0.277	0.028	133.6
1	0.073	0.389	0.039	(2013–7-
0.5	0.048	0.016	0.002	22)
3	0.077	0.233	0.023	69.0
1	0.060	0.395	0.040	(2014–8-
0.5	0.038	0.124	0.012	7)
3	0.023	–	–	23.8
1	0.012	–	–	(2014–8-
0.5	0.008	–	–	9)
3	0.035	0.092	0.009	20.8
1	0.019	0.135	0.013	(2014–8-
0.5	0.012	0.026	0.003	31)
3	0.038	0.005	0.000	60.5
1	0.019	0.013	0.001	(2014–9-
0.5	0.012	–	–	12)
3	0.048	0.008	0.001	69.6
1	0.022	0.027	0.003	(2014–9-
0.5	0.010	–	–	17)
3	0.038	0.007	0.001	31.4
1	0.023	0.023	0.002	(2014–9-
0.5	0.009	–	–	28)

Table 2
Fine root biomass, grain yield, soil moisture, soil temperature, SOC and accumulated respiration for the three slope positions and gradients.

Slope gradient (°)	Slope position	Fine root biomass ($kg\,m^{-2}$)	Grain yield ($kg\,m^{-2}$)	Mean soil moisture (% WFPS)	Mean soil temperature (°C)	SOC ($g\,kg^{-1}$)	Accumulated Respiration ($g\,C\,m^{-2}\,y^{-1}$)	Year
3	Upper	0.32a	0.56a	39.5 ± 10.2b	13.9 ± 0.5a	–	610.3 ± 84.1c	2014
	Middle	0.33a	0.57a	42.6 ± 9.6ab	13.7 ± 0.4a	–	692.2 ± 59.3b	
	Bottom	0.36a	0.59a	45.5 ± 11.3a	13.8 ± 0.6a	–	787.3 ± 94.7a	
	Average	0.33	0.58	42.6 ± 10.5	13.8 ± 0.5	–	658.4 ± 80.8	
1	Upper	0.34a	0.63a	42.2 ± 8.6c	14.3 ± 1.0a	–	698.2 ± 86.4c	
	Middle	0.36a	0.66a	44.1 ± 10.8b	14.9 ± 0.8a	–	814.7 ± 55.5b	
	Bottom	0.37a	0.68a	46.2 ± 9.3a	14.2 ± 0.6a	–	862.4 ± 84.7a	
	Average	0.36	0.66	44.2 ± 9.6	14.5 ± 0.8	–	745.0 ± 71.3	
0.5	Upper	0.43a	0.72a	43.7 ± 12.6a	14.7 ± 0.4a	–	864.0 ± 87.6c	
	Middle	0.38a	0.69a	44.8 ± 9.4a	14.8 ± 0.9a	–	932.6 ± 76.4b	
	Bottom	0.44a	0.65a	45.6 ± 10.7a	15.3 ± 1.2a	–	965.3 ± 65.9a	
	Average	0.42	0.69	46.2 ± 10.1	14.9 ± 0.6	–	868.5 ± 78.1	
3	Upper	0.31a	0.34a	35.8 ± 9.1c	13.4 ± 0.7a	8.2 ± 0.8b	533.1 ± 98.4c	2015
	Middle	0.33a	0.35a	38.4 ± 8.5b	13.3 ± 0.9a	9.1 ± 0.6a	605.2 ± 65.3b	
	Bottom	0.34a	0.38a	42.7 ± 12.0a	13.6 ± 0.6a	9.1 ± 1.1a	656.0 ± 105.6a	
	Average	0.32	0.36	39.0 ± 9.4	13.4 ± 0.7	8.8 ± 0.8	598.1 ± 862.8	
1	Upper	0.32a	0.31a	37.6 ± 7.8c	14.1 ± 1.1a	9.0 ± 0.3b	630.8 ± 68.1c	
	Middle	0.33a	0.41a	40.3 ± 9.7b	14.0 ± 0.8a	10.0 ± 0.5a	753.2 ± 84.0b	
	Bottom	0.35a	0.42a	43.7 ± 10.3a	14.0 ± 0.6a	10.1 ± 0.9a	770.3 ± 75.1a	
	Average	0.33	0.38	40.3 ± 9.1	14.0 ± 0.4	9.6 ± 0.6	717.0 ± 75.9	
0.5	Upper	0.37a	0.40a	41.6 ± 9.5ab	14.6 ± 0.5a	10.2 ± 1.6a	785.6 ± 61.8c	
	Middle	0.34a	0.42a	39.0 ± 10.2b	14.7 ± 0.8a	9.7 ± 0.5a	749.1 ± 89.1b	
	Bottom	0.35a	0.36a	43.2 ± 11.0a	15.0 ± 0.4a	9.9 ± 0.8a	922.8 ± 82.6a	
	Average	0.35	0.39	43.3 ± 10.1	14.7 ± 0.6	9.9 ± 0.9	818.9 ± 76.6	

2014 refers to the period from October 1, 2013 to September 30, 2014; 2015 refers to the period from October 1, 2014 to September 30, 2015. Different letters indicate significant differences at $P < 0.05$.

3.2. Soil moisture, temperature, crop yield and root biomass

The soil moisture on the slopes with different gradients showed similar temporal variations over the two-year experimental period (Fig. 3c). The mean annual soil moisture reached a maximum of 46.2% WFPS in 2014 and 43.3% WFPS in 2015 at $S_{0.5}$, and a minimum of 42.6% WFPS in 2014 and 39.0% WFPS in 2015 at S_3, respectively (Table 2). There was no significant difference in the mean soil moisture among the three slope positions at $S_{0.5}$, while that at S_1 and S_3 decreased in the order of bottom > middle > upper ($P < 0.05$; Table 2). Soil temperatures at 5 cm depth at $S_{0.5}$, S_1 and S_3 also exhibited very similar temporal patterns over the two-year experimental period ($P > 0.05$; Fig. 3b), which was in good agreement with that of air temperature (Fig. 3a). There was no significant difference in the mean soil temperature at $S_{0.5}$, S_1 and S_3 ($P > 0.05$; Table 2).

There was a significant difference in the mean fine root biomass and crop yield among the three slope gradients ($S_{0.5} > S_1 > S_3$, $P < 0.05$; Table 2), but no difference among the three slope positions ($P > 0.05$; Table 2).

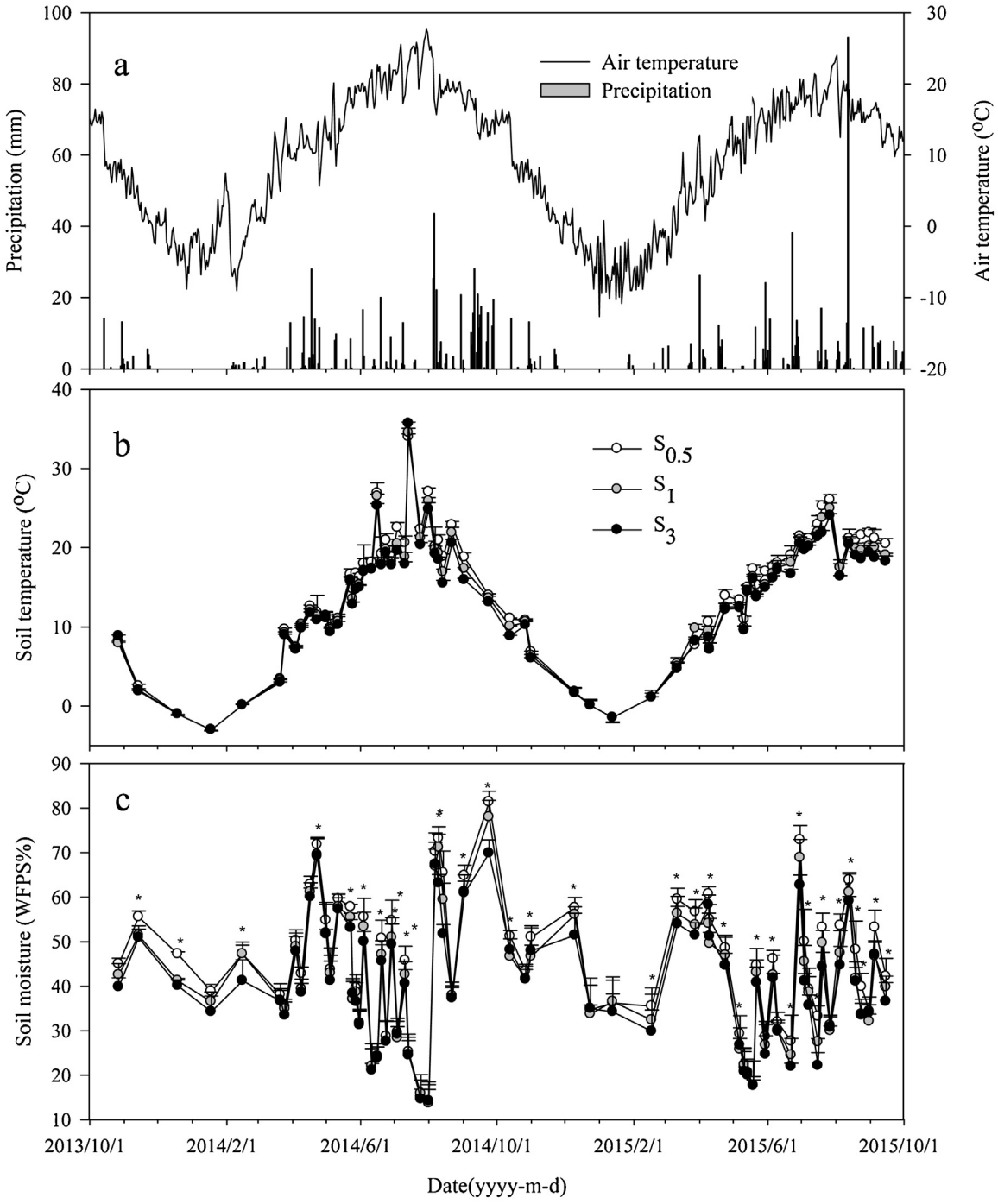

Fig. 3. Variations of (a) precipitation (mm) and air temperature (°C), (b) soil temperature (°C), and (c) soil moisture (% WFPS) from 2014 to 2015. Asterisks indicate significant differences at $P < 0.05$.

3.3. CO_2 emissions under different slope gradients and positions

The CO_2 emissions at $S_{0.5}$, S_1 and S_3 showed similar seasonal and annual patterns (Fig. 4). Specifically, CO_2 emissions increased gradually with increasing temperature before summer from January to June, fluctuated significantly in summer from July to September due to frequent and heavy rainfall and high temperature (Figs. 4 and 3a), and then decreased quickly with decreasing temperature after October.

Slope gradient had a significant effect on soil CO_2 emissions ($P < 0.01$) (Table 2; Fig. 4). In 2014, the mean annual cumulative CO_2 emissions at S_1 and S_3 (731.0 and 628.3 g C m^{-2} $year^{-1}$) were about 13.4% and 25.5% lower than that at $S_{0.5}$ (843.7C m^{-2} $year^{-1}$), and the annual mean CO_2 emissions at S_1 and S_3 (2.64 and 2.38 μmol m^{-2} s^{-1}; Table 1) were 14.8% and 23.2% lower than that at $S_{0.5}$ (3.10 μmol m^{-2} s^{-1}), respectively. A similar trend was also observed in 2015 (Fig. 4).

Slope position also had a significant effect on soil CO_2 emissions ($P < 0.01$) (Table 2; Fig. 5). In general, the CO_2 emissions at different slope positions followed the order of bottom > middle > upper in 2014 and 2015 (Fig. 5).

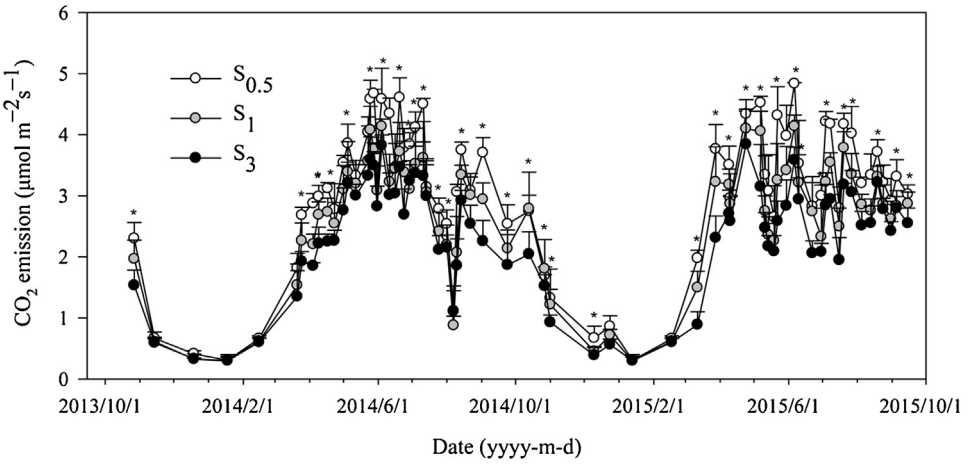

Fig. 4. Dynamics of the CO_2 emission rate (μmol m^{-2} s^{-1}) from 2014 to 2015 in the plots with different gradients. Asterisks indicate significant differences at $P < 0.05$.

4. Discussion

4.1. Effects of slope gradients on CO_2 emissions

Soil CO_2 emissions decreased significantly with the increase of slope gradients (Table 2), which can probably be attributed to the following three reasons: 1) the reduction in soil moisture due to runoff loss on the slopes with greater gradients (Table 2). Under the same natural precipitation (Table 1; Fig. 3a, c), more runoff was generated and discharged at S_3 due to the greater slope gradient (Table 1), and thus less water was retained in the plot. On the contrary, the gentle gradient ($S_{0.5}$) allowed for more efficient downward infiltration (Fox and Bryan, 2000), resulting in less runoff loss (Table 1), and consequently higher soil moisture at the slopes with a gentle gradient. Although there was only a marginal difference in soil moisture among the three slope gradients (Table 2), the negative quadratic correlation between soil moisture and cumulative CO_2 emissions in Figs. 6 and 7 suggested that even a slight increase in soil moisture could have a significant effect on CO_2 emissions, especially when it was neither too dry (WFPS < 20%) nor too wet (WFPS > 60%). Li et al. (2015a) also observed a decrease of CO_2 emissions with increasing slope gradients on much steeper slopes and attributed it to the loss of soil moisture. 2) The variations of CO_2 emissions on different slopes can also be attributed to the significant increase of fine roots and crop yields on the gentler slopes (Table 2). The higher fine root biomass at $S_{0.5}$ (Table 2), where there was less soil and SOC loss, could also lead to more autotrophic CO_2 emissions (Wang et al., 2015a; Zhang et al., 2015b). The higher crop yield at $S_{0.5}$ (Table 2) provided abundant substrates for microbial activities, thereby inducing more heterotrophic CO_2 emissions (Aanderud et al., 2011; Balogh et al., 2011; Jia and Liu, 2017); 3) The decrease of SOC on the steeper slopes induced by erosion was also a reason to induce less CO2 emissions on steeper slopes (Table 2). At the beginning of this long-term experiment since 1998, the SOC content was supposed to be comparable among the three slopes (9.53 g kg^{-1} in Section 2.2.1). However, after nearly two decades of erosion (Table 1) and discharge out of the plots, SOC distribution on each plot were evidently different (9.9 g kg^{-1} at $S_{0.5}$ *vs.* 8.8 g kg^{-1} at S_3) (Table 2). This can be reflected by the increasing runoff and sediment discharge (Table 1), and consequently the SOC content decreased with increasing slope gradient (Table 2). Fine root biomass and grain yield may also contribute to refilling SOC pools (Upson and Burgess, 2013). The decrease of fine root biomass and grain yield (Table 2) further indicated the net loss of SOC over the two decades of erosion. Thus, the significantly less annual CO_2 emissions at S_3 was in part related to its smaller SOC content (Table 2).

The insignificant differences of soil temperature among different slopes (Fig. 3) were probably because all the plots in this study were east-facing. While some studies reported that soil temperature is a major factor controlling soil CO_2 emissions (Eberwein et al., 2015; Reynolds et al., 2015), other reports also stated that no significant difference in soil temperature was observed between the steep and gentle slopes in Moscow oblast (Shein et al., 2011). In this study, given the same orientation of all the slopes and their gentle gradients, soil temperature was not considered as a major factor influencing the differences of soil CO_2 emissions at different slope gradients and positions.

4.2. Effects of slope positions on CO_2 emissions

Erosion-induced spatial redistribution of the soil moisture and SOC resulted in a significant difference in CO_2 emissions among different slope positions (Table 2, Fig. 5) (Fiener et al., 2012). On such gentle slopes as in this study ($S_{0.5}$, S_1 and S_3), soil erosion was predominantly the interrill erosion, which was associated with selective entrainment and transport of fine/light particles and associated substances (e.g., SOC, P, N and clay) (Hu et al., 2013; Kuhn and Armstrong, 2012; Schiettecatte et al., 2008). After decades of selective erosion, SOC was gradually eroded away from the upper slope and then deposited at lower positions, resulting in decreased SOC at upper positions and enriched SOC at lower positions (Table 2). However, such lateral spatial redistribution of SOC along the slope was less evident on the gentler slopes (Table 2), probably because the slope with a gentle gradient ($S_{0.5}$) did not suffer from substantial erosion and transport of soil particles (Table 1).

In the rain-fed areas of the semi-arid Loess Plateau, the soil moisture at a certain point on the slope M was calculated from the following equation:

$$M = M_{antecedent} + M_{precipitation} + M_{inflow} - M_{outflow} - E \quad (2)$$

where $M_{antecedent}$ is the antecedent moisture content at a certain point from previous scenarios, $M_{precipitation}$ is the water received directly from natural precipitation, M_{inflow} is the water received indirectly from the inflow of upper slope positions, $M_{outlfow}$ is the water that flows into lower slope positions, and E is the evaporation. In this study, the three east-facing slopes had the same natural precipitation and soil temperature (Table 2), thus $M_{precipitation}$ and E can be assumed comparable among the three slope gradients. However, slope position may have an effect on M_{inflow} and $M_{outflow}$, especially at the upper and lower positions.

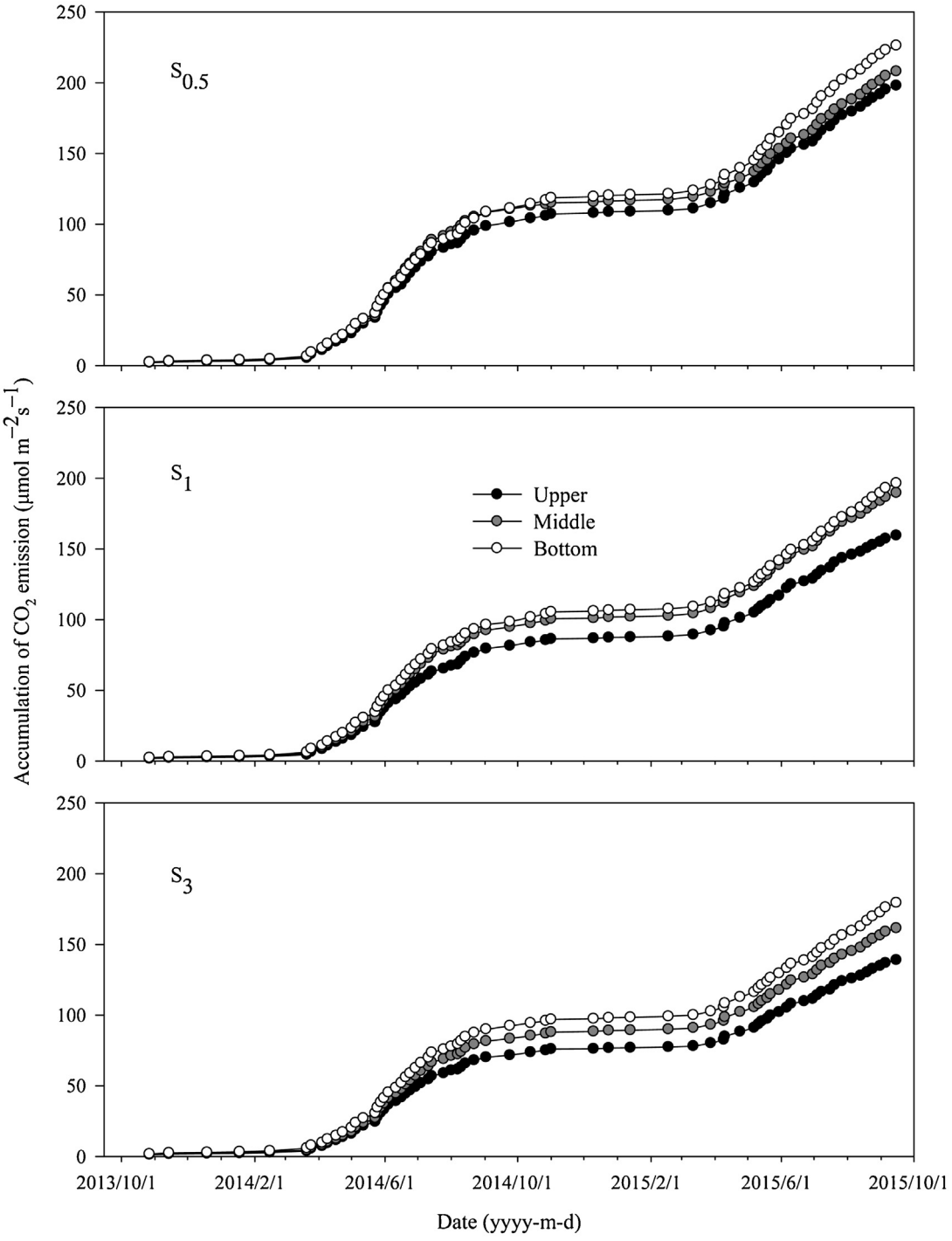

Fig. 5. Dynamics of the accumulation CO_2 emissions rate ($\mu mol\, m^{-2}\, s^{-1}$) from 2014 to 2015 at different slope positions.

In this study, all the plots were filled with soil (0–20 cm) obtained from local cropland, and soil moisture was maintained to be 12–15%. After each precipitation event, the water on the slope was redistributed by gravity in two directions: laterally downward the slope via runoff and vertically into subsoil via infiltration, resulting in the loss of soil water at upper positions and the accumulation of soil water at lower positions. The redistribution of water would be intensified after repeated precipitation events, resulting in significant differences in soil moisture content among different slope positions, especially between the upper and lower positions (Table 2). As a result, it may be inappropriate to use the average of soil moisture contents obtained from different slope positions to estimate the CO_2 emissions from sloping land.

5. Conclusions

Soil CO_2 emissions significantly decreased with the increase of slope gradient, but increased from the upper slope to the bottom slope, which could be attributed mainly to the spatial redistribution of soil moisture and SOC induced by erosion, and consequently varying fine root biomass across different slope gradients and positions. Therefore, slope gradients and positions should be considered

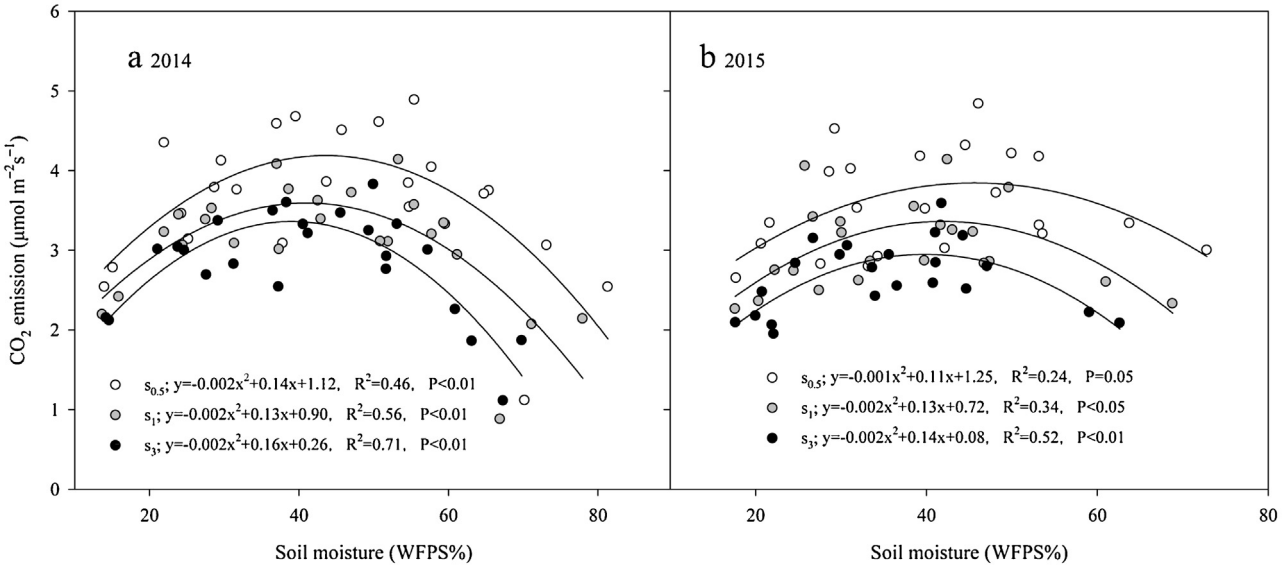

Fig. 6. Relationship between soil CO_2 emission rate ($\mu mol\ m^{-2}\ s^{-1}$) and soil moisture (%WFPS) at 0–5 cm depth at different slope gradients from May to September (temperatures were above 10 °C). White indicates $S_{0.5}$, Gray indicates S_1, Black indicates S_3.

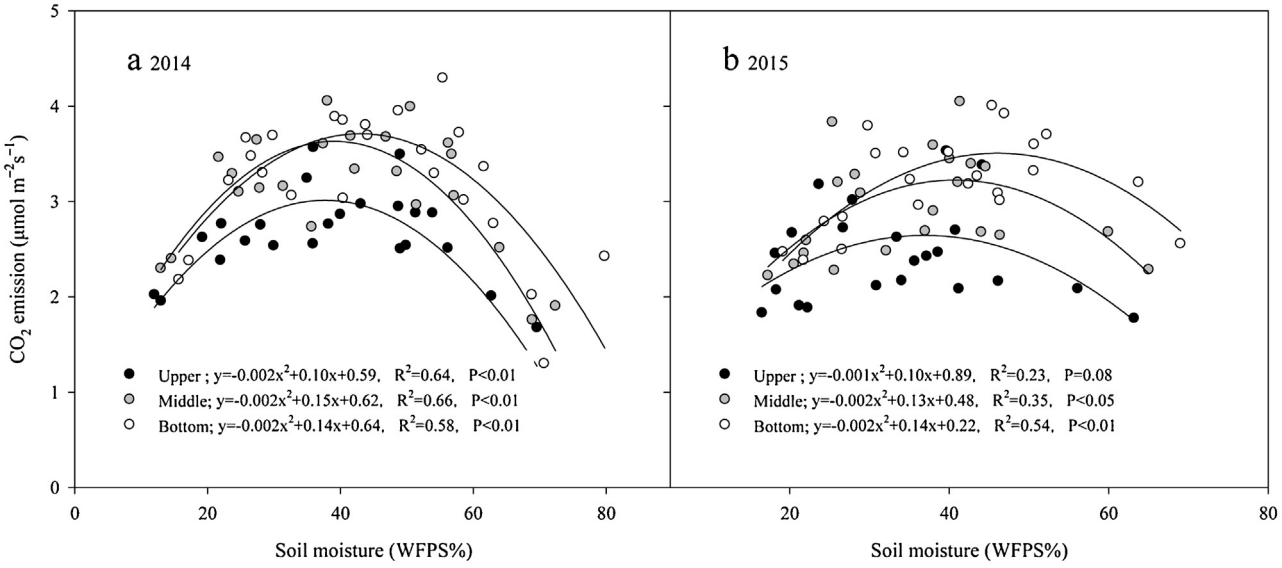

Fig. 7. Relationship between soil CO_2 emission rate ($\mu mol\ m^{-2}\ s^{-1}$) and soil moisture (%WFPS) at 0–5 cm depth at different slope positions from May to September (temperatures were above 10 °C). White indicates Bottom, Gray indicates Middle, Black indicates upper.

in estimating soil CO_2 emissions and carbon cycling in the complex and fragmented topography regions.

Acknowledgement

This work is supported by Natural Science Foundation of China (No. 41371279) and Fundamental Research Funds of Northwest A&F University (Z109021712).

References

Aanderud, Z., Schoolmaster, D., Lennon, J., 2011. Plants mediate the sensitivity of soil respiration to rainfall variability. Ecosystems 14, 156–167.
Balogh, J., Pintér, K., Fóti, S., Cserhalmi, D., Papp, M., Nagy, Z., 2011. Dependence of soil respiration on soil moisture, clay content, soil organic matter, and CO_2 uptake in dry grasslands. Soil Biol. Biochem. 43, 1006–1013.
Berhe, A., Kleber, M., 2013. Erosion, deposition, and the persistence of soil organic matter: mechanistic considerations and problems with terminology. Earth Surf. Proc. Land 38, 908–912.
Bond-Lamberty, B., Thomson, A., 2010. Temperature-associated increases in the global soil respiration record. Nature 464, 579–582.
Chen, S., Xu, J., Wang, W., 2009. The research on erosional types and process of head-cut on Dongzhiyuan of Loess Plateau. Chin. Agric. Sci. Bull. 25, 258–263.
Chen, G., Xu, M., Zhang, Y., Wang, C., Fan, H., Wang, S., 2015. Characteristics of soil respiration along eroded sloping Land with different SOC background on the hilly Loess Plateau. Environ. Sci. 36, 3383–3392.
Eberwein, J.R., Oikawa, P.Y., Allsman, L.A., Jenerette, G.D., 2015. Carbon availability regulates soil respiration response to nitrogen and temperature. Soil Biol. Biochem. 88, 158–164.
Fehmi, J.S., Kong, T.M., 2012. Effects of soil type, rainfall, straw mulch, and fertilizer on semi-arid vegetation establishment growth and diversity. Ecol. Eng. 44, 70–77.
Fereidoonia, M., Raiesi, F., Fallah, S., 2013. Ecological restoration of soil respiration, microbial biomass and enzyme activities through broiler litter application in a calcareous soil cropped with silage maize. Ecol. Eng. 58, 266–277.
Fiener, P., Dlugo, V., Korres, W., Schneider, K., 2012. Spatial variability of soil respiration in a small agricultural watershed –are patterns of soil redistribution important? Catena 94, 3–16.
Fox, D., Bryan, R., 2000. The relationship of soil loss by interrill erosion to slope gradient. Catena 38, 211–222.

Hu, Y., Fister, W., Kuhn, N., 2013. Temporal variation of SOC enrichment from interrill erosion over prolonged rainfall simulations. Agriculture 3, 726–740.
Hursh, A., Ballantyne, A., Cooper, L., Maneta, M., Kimball, J., Watts, J., 2017. The sensitivity of soil respiration to soil temperature, moisture, and carbon supply at the global scale. Glob. Change Biol. 23, 2090–2103.
Jia, G., Liu, X., 2017. Soil microbial biomass and metabolic quotient across a gradient of the duration of annually cyclic drainage of hillslope riparian zone in the three gorges reservoir area. Ecol. Eng. 99, 366–373.
Jiang, J., Guo, S., Zhang, Y.J., Liu, Q., Wang, R., Wang, Z., Li, N., Li, R., 2015. Changes in temperature sensitivity of soil respiration in the phases of a three-year crop rotation system. Soil Tillage Res. 150, 139–146.
Kuhn, N., Armstrong, E., 2012. Erosion of organic matter from sandy soils: solving the mass balance. Catena 98, 87–95.
Li, R., Zhang, Y., Zhao, M., Du, L., Wang, Z., Guo, S., 2015a. Effects of slope and rainfall on soil CO_2 flux and SOC Loss under simulation experiment. Acta Scientiae Circumstantiae 36, 1336–1342.
Li, X., Li, Y., Yu, H., Zhang, Y., Guo, Z., 2015b. Spatial changes in soil CO_2 emission from re-forested hillslopes on the Loess Plateau: a geomorphic control. J. Plant Nutr. Fertil. 21, 1217–1224.
Liu, J., Wang, D., Lei, R., Wu, Q., 2004. Fine roots biomass and spatial dynamic in the *Natural stands of sharptooth oak chinese pine* at huoditang forest region. J. Northwest For. Univ. 19, 1–4.
Liu, T., Xu, Z., Hou, Y., Zhou, G., 2016. Effects of warming and changing precipitation rates on soil respiration over two years in a desert steppe of northern China. Plant Soil 400, 15–27.
Makita, N., Pumpanen, J., Köster, K., Berninger, F., 2016. Changes in very fine root respiration and morphology with time since last fire in a boreal forest. Plant Soil 402, 303–316.
Pandey, V.C., Sahu, N., Behera, S.K., Singh, N., 2016. Carbon sequestration in fly ash dumps: comparative assessment of three plant association. Ecol. Eng. 100, 291–300.
Pei, H., Xu, M., Tuo, D., 2012. Effects of erosion on slopeland in the Loess hilly region. Bull. Soil Water Conserv. 32, 1–4.
Reynolds, L., Johnson, B., Pfeifer-Meister, L., Bridgham, S., 2015. Soil respiration response to climate change in Pacific Northwest prairies is mediated by a regional Mediterranean climate gradient. Glob. Change Biol. 21, 487–500.
Schiettecatte, W., Gabriels, D., Cornelis, W., Hofman, G., 2008. Enrichment of organic carbon in sediment transport by interrill and rill erosion processes. Soil Sci. Soc. Am. J. 72, 50–55.
Shein, E.V., Bannikov, M.V., Savoskina, O.A., Mazirov, M.A., 2011. Temperature regime of agrosoddy podzolic soils on slopes of different steepness. Eurasian Soil Sci. 44, 157–162.
Singh, R., Singh, H., Singh, S., Afreen, T., Upadhyay, S., Singh, A.K., Srivastava, P., Bhadouria Rahul Raghubanshi, A.S., 2017. Riparian land uses affect the dry season soil CO2 efflux under dry tropical ecosystems. Ecol. Eng. 95, 198–205.
Sparks, D.L., Page, A.L., Helmke, P.A., Loeppert, R.H., Soltanpour, P.N., Johnston, C.T., Sumner, M.E., 1996. Methods of Soil Analysis. Part 3. Chemical Methods Soil Science Society of America Inc, Madison, WI.
Tang, J., Qi, Y., Xu, M., Misson, L., Goldstein, A., 2005. Forest thinning and soil respiration in a ponderosa pine plantation in the Sierra Nevada. Tree Physiol. 25, 57–66.
Upson, M., Burgess, P., 2013. Soil organic carbon and root distribution in a temperate arable agroforestry system. Plant Soil 373, 43–58.
Van Hemelryck, H., Govers, G., Van Oost, K., Merckx, R., 2011. Evaluating the impact of soil redistribution on the in situ mineralization of soil organic carbon. Earth Surf. Proc. Landf. 36, 427–438.
Van, H., Fiener, P., Van, K., Govers, G., Merckx, R., 2010. The effect of soil redistribution on soil organic carbon: an experimental study. Biogeosciences 7, 3971–3986.
Wang, R., Guo, S., Jiang, J., Wu, D., Li, N., Zhang, Y., Liu, Q., Li, R., Wang, Z., Sun, Q., Du, L., Zhao, M., 2015a. Tree-scale spatial variation of soil respiration and its influence factors in apple orchard in Loess Plateau. Nutr. Cycl. Agroecosyst. 102, 285–297.
Wang, Z., Guo, S., Sun, Q., Li, N., Jiang, J., Wang, R., Zhang, Y., Liu, Q., Wu, D., Li, R., Du, L., Zhao, M., 2015b. Soil organic carbon sequestration potential of artificial and natural vegetation in the hilly regions of Loess Plateau. Ecol. Eng. 82, 547–554.
Wei, S., Zhang, x., Mclaughlin, N.B., Liang, A., Jia, S., Chen, X., Chen, X., 2014. Effect of soil temperature and soil moisture on CO2 flux from eroded landscape positions on black soil in Northeast China. Soil Tillage Res. 144, 119–125.
Xiao, L., Yang, X., Chen, S., Cai, H., 2015. An assessment of erosivity distribution and its influence on the effectiveness of land use conversion for reducing soil erosion in Jiangxi, China. Catena 125, 50–60.
Zhang, L., Gao, Z., Yang, S., Li, Y., Tian, H., 2015a. Dynamic processes of soil erosion by runoff on engineered landforms derived from expressway construction: a case study of typical steep spoil heap. Catena 128, 108–121.
Zhang, Y., Guo, S., Liu, Q., Jiang, J., Wang, R., Li, N., 2015b. Responses of soil respiration to land use conversions in degraded ecosystem of the semi-arid Loess Plateau. Ecol. Eng. 74, 196–205.
Zhao, Q., Li, D., Zhou, M., Guo, T., Liao, Y., Xie, Z., 2015. Effects of rainfall intensity and slope gradient on erosion characteristics of the red soil slope. Stoch. Env. Res. Risk A 29, 609–621.
Zhu, H., Wu, J., Guo, S., Huang, D., Zhu, Q., Ge, T., Lei, T., 2014. Land use and topographic position control soil organic C and N accumulation in eroded hilly watershed of the Loess Plateau. Catena 120, 64–72.